$$= \frac{G^2}{2\pi M^2} \frac{E'}{E} \left(\cos^2 \theta/2 \, W_2^{\nu,\bar{\nu}} + 2 \sin^2 \theta/2 \, W_1^{\nu,\bar{\nu}} \mp \frac{E+E'}{M} \sin^2 \theta/2 \, W_3^{\nu,\bar{\nu}} \right) + 0(m^2) \qquad (2.11)$$

where θ is the angle between the directions of the initial and final leptons in the laboratory. The final lepton's polarization is given by:

$$P^L_{\nu,\bar{\nu}} = \mp \left| \pm \frac{m^2 \left(2W_1 \cos^2 \frac{\theta}{2} + W_2 \sin^2 \frac{\theta}{2} \mp W_3 \frac{(E-E')}{M} \cos^2 \frac{\theta}{2} + \frac{4E'^2}{M^2} \sin^2 \frac{\theta}{2} W_4 - \frac{2E'}{M} \sin^2 \frac{\theta}{2} W_5 \right)}{2E'^2 \left(2W_1 \sin^2 \frac{\theta}{2} + W_2 \cos^2 \frac{\theta}{2} \mp \frac{(E+E')}{M} \sin^2 \frac{\theta}{2} W_3 \right)} \right. + 0(m^2)$$

$$P^P_{\nu,\bar{\nu}} = \pm \frac{m \sin\theta \left(2W_1 - W_2 + \frac{W_5 E'}{M} \pm \frac{W_3 E}{M} \right)}{2E' \left(\cos^2 \frac{\theta}{2} W_2 + 2 \sin^2 \frac{\theta}{2} W_1 \mp \frac{E+E'}{M} \sin^2 \frac{\theta}{2} W_3 \right)} + 0\,(m^2) \qquad (2.12)$$

$$P^T_{\nu,\bar{\nu}} = - \frac{m}{M} \sin\theta \frac{2W_6}{2W_1 \sin^2 \frac{\theta}{2} + W_2 \cos^2 \frac{\theta}{2} \mp \frac{E+E'}{M} \sin^2 \frac{\theta}{2} W_3} + 0\,(m^2)$$

where the longitudinal (L), perpendicular (P), and transverse (T) polarization vectors have been chosen so that their space components are orthogonal in the laboratory frame and satisfy

$$\begin{aligned} \vec{S}^L &\alpha \vec{k}' \\ \vec{S}^T &\alpha \vec{k} \times \vec{k}' \\ \vec{S}^P &\alpha \vec{S}^L \times \vec{S}^T \,. \end{aligned} \qquad (2.13)$$

It may be that at high energies the factorization of $\mathscr{L}_{\text{eff}}$ into leptonic and hadronic parts still obtains but the exchange of other spins plays a role. Generally, if spin J is exchanged the invariant matrix element squared, summed over spins, etc., will be a $2J^{\text{th}}$ order polynomial in $\cos\theta_t$ (2.8). A direct test for scalar and tensor currents is that they cause the helicity of the final lepton

to be opposite to that of the initial neutrino in the approximation m = 0; with only vector and/or axial vector currents, the helicity is unchanged if m = 0. Cheng and Tung have discussed other tests for the presence of scalar and tensor currents.(C16)

The general theorems discussed here are all violated by electromagnetic effects. It might be feared that with a nuclear target of charge Z, corrections of order $Z\alpha$ could occur. Nachtmann has studied this problem(N1), and has shown that the corrections to Eq. (2.7) are characterized by $Z\alpha/E'R$, where E' is the energy of the outgoing lepton and R is the nuclear radius. Nachtmann finds corrections $\lesssim$ 5% in uranium.

2.2. Tests of properties of the hadron current

A. Selection Rules

$\Delta Y \leq 1$ and $\Delta Y = \Delta Q$

The simplest reactions forbidden by these selection rules are listed in Table 2. The branching ratios for the "forbidden" processes depend on the square of the violation parameter (y). Roe has pointed out(R8) that K^o production provides a test which is linear in y, since

$$\bar{\nu} p \longrightarrow \mu^+ \Lambda^o (K^o + y\bar{K}^o) \qquad (y = 0 \text{ if } \Delta Y \leq 1 \text{ only})$$

$$\nu n \longrightarrow \mu^- p (K^o + y'\bar{K}^o) \qquad (y' = 0 \text{ if } \Delta Y = \Delta Q \text{ only})$$

If $y/y' \neq 0$, the observed states K_S and K_L occur in unequal numbers and this can be detected in a suitable apparatus.

$\Delta I = 1/2$ in $\Delta Y = 1$ transitions

For the reactions involving a single baryon or baryon resonance with I = 1 in the final state, this rule gives(L13):

$$\frac{\sigma(\bar{\nu} n \longrightarrow \Sigma^-)}{\sigma(\bar{\nu} p \longrightarrow \Sigma^o)} = \frac{\sigma(\bar{\nu} n \longrightarrow Y^{*-})}{\sigma(\bar{\nu} p \longrightarrow Y^{*o})} = 2 . \qquad (2.14)$$

In Eq. (2.14) and below, the presence of the appropriate lepton in the final state is understood. In reactions with two stable hadrons in the final state we find:

$$\frac{\sigma(\bar{\nu}n \to \Sigma^o \pi^-)}{\sigma(\bar{\nu}n \to \Sigma^- \pi^o)} = 1$$

$$\frac{\sigma(\bar{\nu}n \to \Lambda^o \pi^-)}{\sigma(\bar{\nu}p \to \Lambda^o \pi^o)} = \frac{\sigma(\bar{\nu}n \to \Sigma^- \eta^o)}{\sigma(\bar{\nu}p \to \Sigma^o \eta^o)} = 2 \qquad (2.15)$$

The $\Delta I = 1/2$ rule also gives a number of "triangular inequalities" for this class of reactions.[L13] The "triangular inequalities" between quantities σ_1, σ_2, and σ_3 are defined to be:

$$\sqrt{\sigma_1} + \sqrt{\sigma_2} \geq \sqrt{\sigma_3}$$

$$\sqrt{\sigma_1} + \sqrt{\sigma_3} \geq \sqrt{\sigma_2} \qquad (2.16)$$

$$\sqrt{\sigma_2} + \sqrt{\sigma_3} \geq \sqrt{\sigma_1}$$

The triplets $\sigma_{1,2,3}$ for which these inequalities hold are:

σ_1	σ_2	σ_3
$\sigma(\nu p \to pK^+)$	$\sigma(\nu n \to pK^o)$	$\sigma(\nu n \to nK^+)$
$\sigma(\bar{\nu}n \to \Xi^- K^o)$	$\sigma(\bar{\nu}p \to \Xi^o K^o)$	$\sigma(\bar{\nu}p \to \Xi^- K^+)$
$\sigma(\bar{\nu}n \to nK^-)$	$\sigma(\bar{\nu}p \to n\bar{K}^o)$	$\sigma(\bar{\nu}p \to pK^-)$
$2\sigma(\bar{\nu}n \to \Sigma^o \pi^o)$	$\sigma(\bar{\nu}p \to \Sigma^+ \pi^-)$	$\sigma(\bar{\nu}p \to \Sigma^- \pi^+)$
$2\sigma(\bar{\nu}p \to \Sigma^o \pi^o)$	$\sigma(\bar{\nu}p \to \Sigma^+ \pi^-)$	$\sigma(\bar{\nu}p \to \Sigma^- \pi^+)$

(2.17)

$|\Delta I = 1|$ for $\Delta Y = 0$ Transitions

This rule gives

$$\frac{\sigma(\nu p \to N^{*++})}{\sigma(\nu n \to N^{*+})} = \frac{\sigma(\bar{\nu} n \to N^{*-})}{\sigma(\bar{\nu} p \to N^{*0})} = 3 \qquad (2.18)$$

and triangular inequalities (cf. Eq. 2.16) for:

σ_1	σ_2	σ_3
$2\sigma(\nu n \to p\pi^0)$	$\sigma(\nu p \to p\pi^+)$	$\sigma(\nu n \to n\pi^+)$
$2\sigma(\nu n \to \Sigma^0 K^+)$	$\sigma(\nu p \to \Sigma^+ K^+)$	$\sigma(\nu n \to \Sigma^+ K^0)$
$2\sigma(\bar{\nu} p \to n\pi^0)$	$\sigma(\bar{\nu} n \to n\pi^-)$	$\sigma(\bar{\nu} p \to p\pi^-)$
$2\sigma(\bar{\nu} p \to \Sigma^0 K^0)$	$\sigma(\bar{\nu} n \to \Sigma^- K^0)$	$\sigma(\bar{\nu} p \to \Sigma^- K^+)$

(2.19)

Charge symmetry of the $\Delta Y = 0$ current

The charge symmetry condition (1.3) relates the form factors in pairs of processes such as $\nu_\mu p \to \mu^- p \pi^+$ and $\bar{\nu}_\mu n \to \mu^+ n \pi^-$, for example. Note that it does not give equal cross sections since the ν and $\bar{\nu}$ currents are different. If the lepton spins are summed over, however, the lepton tensor is unchanged when $\nu \longleftrightarrow \bar{\nu}$ except that the V-A interference term changes sign. Therefore, for $\Delta Y = 0$ reactions

$$\sum_{\substack{\text{lepton}\\ \text{spins}}} \left[d\sigma \begin{pmatrix} \nu p \to \mu^- a\,(I_3 = 3/2) \\ \nu n \to \mu^+ b\,(I_3 = 1/2) \end{pmatrix} - d\sigma \begin{pmatrix} \bar{\nu} n \to \mu^+ a\,(I_3 = -3/2) \\ \bar{\nu} p \to \mu^+ b\,(I_3 = -1/2) \end{pmatrix} \right]$$

is proportional to the V-A interference term.

If all final states are summed over, the charge symmetry condition gives:

$$W_i^{\nu p} = W_i^{\bar{\nu} n}$$
$$(\Delta Y = 0) \qquad (2.20)$$
$$W_i^{\bar{\nu} p} = W_i^{\nu n}$$

for the W_i (Eq. 2.5). This gives obvious relations between (e.g.) the cross sections for ν and $\bar{\nu}$ on deuterium. For the quasi-elastic process the charge symmetry condition is:

$$\langle p \left| J_\lambda^{0+} \right| n \rangle = - \langle n \left| J_\lambda^{0-} \right| p \rangle \qquad (2.21)$$

which, combined with the identity $\langle p \left| J_\lambda^{0+} \right| n \rangle^* = \langle n \left| J_\lambda^{0-} \right| p \rangle$, gives strong restrictions (see Section 3.3).

Absence of second-class currents

This hypothesis is the same as the charge symmetry condition if the $\Delta Y = 0$ semileptonic part of $\mathscr{L}_{eff}$ conserves T, as we saw in Section 1.1D. If T is not conserved, this hypothesis implies phase conditions for form factors--see Section 3.3.

B. CVC and PCAC (Adler's theorem[A3])

An obvious consequence of CVC is that it reduces the number of independent vector form factors, which are then related to form factors measured in electroproduction by the isotriplet current hypothesis. These relations will be extensively exploited in Chapter 3. Here we shall discuss a theorem due to Adler which leads to direct tests of CVC and PCAC.

Consider the case when the lepton continues forward in the direction of the incident neutrino ($\theta = 0$). We shall neglect the lepton's mass so that the lepton and neutrino helicities are the same because of the factor $\gamma_\lambda(1-\gamma_5)$ in the coupling. The spin is therefore conserved when $\theta = 0$ and j_λ can be written as some linear combination of k_λ and k'_λ. With $\theta = 0$, however, $\vec{k} \propto \vec{k'}$ and k_λ and k'_λ are also proportional in the approximation $k'^2 = k^2 = 0$. We can therefore write

$$j_\lambda \propto q_\lambda = k_\lambda - k'_\lambda \qquad (\theta = 0,\ m = 0)\ , \qquad (2.22)$$

unless $q_\lambda = 0$, as it is for elastic scattering in these conditions. Equation (2.22) implies that:

(a) If CVC is correct, then only the axial current contributes when $\theta = 0$. Parity violating effects should therefore vanish in this configuration.

(b) Assuming CVC, the matrix element is proportional to $q_\lambda A_\lambda$. This then implies $\sigma^{\nu}(\theta = 0) \propto \sigma_\pi$, assuming PCAC. Putting in the correct factors we find (in the notation of Eq. 2.1):

$$\left.\frac{M^4 d^2\sigma^{\bar{\nu},\nu\to F}}{d\left|q^2\right| dW^2}\right|_{\theta=0} = \frac{M^2 G^2 \cos^2\theta_c f_\pi^2}{4\pi^2}\,\frac{E'}{E}\,\frac{M^2}{p_\pi W}\,\sigma_{\pi^\pm\to F}(W)\left(1+\frac{q_0 m^2}{2k_0'\left(q^2-M_\pi^2\right)}\right)^2$$

$$= 4.0\times10^{-14}\,\frac{E'}{E}\,\frac{M^2}{p_\pi W}\,\sigma_{\pi^\pm\to F}(W)\left(1+\frac{q_0 m^2}{2k_0'\left(q^2-M_\pi^2\right)}\right)^2 \qquad (2.23)$$

where

$$W^2 = M^2 + q^2 + 2\nu$$

$$q^2\Big|_{\theta=0} = m^2 - 2EE' + 2E\sqrt{E'^2 - m^2}$$

$\sigma_{\pi^\pm\to F}(W)$ = pion cross section for the same target and final state F at center-of-mass energy W.

p_π = pion center-of-mass momentum at center-of-mass energy W.

Following Adler, we have assumed that pion scattering is dominated by p waves in extrapolating to zero mass in Eq. (2.23) (the choice of extrapolation procedure is clearly irrelevant at large energies) and we have retained the lepton mass in the pion pole term which might be important. The numerical constant was obtained using the Goldberger-Treiman value of $f_\pi \left(= \sqrt{2}\, M g_A / g_{NN\pi} \simeq 0.86\, M_\pi\right)$.

The main problem in comparing Eq. (2.23) with experiment is that there are no events with $\theta \equiv 0$ and rapid variations may occur in this neighborhood due to terms which vanish at $q^2 = 0$. One inelastic reaction for which detailed phenomenological descriptions are available which could be fitted to the data at small q^2 and used to extract $\left.\frac{d\sigma}{dq^2}\right|_{\theta=0}$ is N* production. However, the success of Eq. (2.23) for N* production (or single π production) would not necessarily constitute a new test of PCAC. This is because the success of the Goldberger-Treiman relation ensures that Adler's theorem is satisfied for the Born term for single pion production. Therefore in most dynamical models of this process, in which both $\sigma(\nu N)$ and $\sigma(\pi N)$ are proportional to the Born terms enchanced in the same way, Adler's theorem is automatically satisfied.

An important point about the comparison of Eq. (2.23) with experiment is that $q^2 \simeq -4EE'\sin^2\frac{\theta}{2}$ is generally a more appropriate variable in which to expand than θ (as has been emphasized by Piketty and Stodolsky[P16]). Therefore, the range of θ for which Eq. (2.23) is a good approximation decreases with increasing EE'. If EE' (and hence q^2) is not known so that Eq. (2.23) can only be compared to experiment for small θ, then the relevant range of θ may be very small since $\left.\frac{d\sigma}{d\cos\theta}\right|_{\theta=0} \sim EE'$. (The actual range of q^2 or θ for which Eq. (2.23) is a good approximation depends on the reaction in question, of course.)

A subtle consequence of Eq. (2.23) is that the forward neutrino cross section should vary with different nuclear targets like the pion cross section[B7,B8] (this is often called the "$A^{2/3}$" law--actually $\sigma_\pi \sim A^{0.75}$ at high energies). Such a phenomenon is by now well known in the electromagnetic case.

Experiments have been done to test these predictions. We shall discuss them and give more details of the theory in Section 3.8 after more phenomenological machinery has been assembled. Here we only remark that the Adler-Weisberger relation can be considered a successful test of Adler's relation for an integral over $\sigma^{\bar{\nu}} - \sigma^{\nu}$ if we accept the current algebra hypothesis.

Current Algebra

The only direct tests of the commutators (1.6 - 1.8) are Adler's sum rules[A5]:

$$\int_0^\infty W_2^{\bar{\nu}}\left((\nu, q^2=0) - W_2^{\nu}(\nu, q^2=0)\right) d\nu = 4 M^2 \cos^2\theta_c \langle I_3\rangle \quad (\Delta Y=0) \quad (2.24)$$

$$\int_0^\infty \left(W_2^{\bar{\nu}}(\nu, q^2=0) - W_2^{\nu}(\nu, q^2=0)\right) d\nu = M^2 \sin^2\theta_c \langle 3Y+2I_3\rangle \quad (\Delta Y=1) \quad (2.25)$$

Separating the quasi-elastic contribution and using Adler's PCAC theorem (2.23), Eq. (2.24) immediately reduces to the celebrated Adler-Weisberger relation. This has been frequently discussed and we will not dwell on the derivation.

Adler has derived sum rules which depend on the commutators (1.3 - 1.5) in unintegrated form, e.g:

$$\left[F_0^k(\vec{x}, 0),\ F_0^\ell(0)\right] = \delta(\vec{x})\, i f^{k\ell m} F_0^m(0)\ , \text{ etc.} \quad (2.26)$$

For two reasons we shall only discuss Adler's so-called β sum rule:

(1) The "α" and "γ" sum rules involve suspect assumptions about high energy behavior which are untrue in free field theories and also in Regge models.

(2) They rely on commutators involving space components of currents which are model dependent. Some such sum rules will be discussed in Section 3.6.

If $W_{\mu\nu}$ (Eq. 2.4) is averaged over initial spins and summed over final states, it may be written in the form:

$$W_{\mu\nu}^{\bar{\nu}} = \bar{\sum}\int \frac{d^4x}{4\pi} e^{iq\cdot x} \langle p\left|\left[J_\mu^+(x),\ J_\nu^-(0)\right]\right|p\rangle \quad (2.27)$$

(The introduction of a commutator in place of $J_\mu^+(x)J_\nu(0)$ is allowed since the extra term only contributes in the unphysical region where $q \cdot P < 0$.) The simplest derivation of the sum rule starts from:

$$\int dq_0 W_{00}^{\overline{\nu}} = \sum \int \frac{d^3x}{2} e^{-i\vec{q}\cdot\vec{x}} \langle p \left| \left[J_0^+(\vec{x}, 0), J_0^-(0) \right] \right| p \rangle$$

$$= \langle 4I_3 \cos^2\theta_c + (3Y+2I_3)\sin^2\theta_c \rangle P_0 M^2. \qquad (2.28)$$

We then write $dq_0 = d\nu / \sqrt{\vec{P}^2 + M^2}$, where $\nu = q \cdot P$ and choose a frame where $\vec{q} \cdot \vec{P} = 0$; note that the integration is at varying $q^2 = \nu^2/(\vec{P}^2 + M^2) - \vec{q}^2$. Finally Eq. (2.28) is divided by P_0 and the limit $|\vec{P}| \longrightarrow \infty$ is taken. Assuming that the limiting process and the integration can be interchanged and using Eq. (2.5) we get the fixed q^2 sum rule

$$\int_{-\infty}^{+\infty} d\nu \; W_2^{\overline{\nu}}(\nu, q^2) = \langle 4I_3 \cos^2\theta_c + (3Y+2I_3)\sin^2\theta_c \rangle M^2 \qquad (2.29)$$

Using the crossing property:

$$W_i^{\nu}(\nu, q^2) = -W_i^{\overline{\nu}}(-\nu, q^2) \quad (i \neq 5), \qquad (2.30)$$

$$\left(W_5^{\nu}(\nu, q^2) = W_5^{\overline{\nu}}(-\nu, q^2) \right),$$

which follows directly from (2.27), Eq. (2.29) may be written in the final form:

$$\int_0^{\infty} \left(W_2^{\overline{\nu}}(\nu, q^2) - W_2^{\nu}(\nu, q^2) \right) d\nu = \langle 4\cos^2\theta_c I_3 + (3Y+2I_3)\sin^2\theta_c \rangle M^2 \qquad (2.31)$$

This equation reduces to (2.24) and (2.25) at $q^2 = 0$. Using Eq. (2.11), (2.31) may be written in the form:

$$E \lim_{\nu \to \infty} \left(\frac{d\sigma^{\overline{\nu}p}}{d|q^2|} - \frac{d\sigma^{\nu p}}{d|q^2|} \right) = \frac{G^2}{\pi} \left(\cos^2\theta_c + 2\sin^2\theta_c \right) \qquad (2.32)$$

$$(m = 0)$$

which suggest a simple interpretation in terms of "point-like" constituents in the nucleon which we shall discuss in Section 3.6.

2.3. T Violation

If time reversal invariance symmetry held then (given the properties of the lepton current under T) it is easy to see that W_6 (Eq. 2.5) would be zero for the quasi-elastic process and for the case when all final states are summed. In the approximation that (2.12) applies $\left(\text{lowest order in G and } \alpha = \frac{e^2}{4\pi} = 0\right) W_6 = 0$ implies that in the laboratory the final lepton has no polarization transverse to the plane in which $\vec{k}$ and $\vec{k}'$ lie.[L11,B15,A2,C2] We shall now derive this result directly.[L25,B5]

If time reversal invariance holds:

$$\begin{aligned} \left|M(\alpha \longrightarrow \beta)\right|^2 &= \langle \alpha \left| T^+ \right| \beta \rangle \quad \langle \beta \left| T \right| \alpha \rangle \\ &= \left|M(\beta' \longrightarrow \alpha')\right|^2 = \langle \beta' \left| T^+ \right| \alpha' \rangle \quad \langle \alpha' \left| T \right| \beta' \rangle \end{aligned} \tag{2.33}$$

where α' and β' are the time reversal states corresponding to α and β (spins and momenta reversed). If in addition the T matrix satisfies $T_{\alpha\beta} = T^+_{\alpha\beta} e^{i\delta\alpha\beta}$ (δ real) then:

$$\left|M(\alpha \longrightarrow \beta)\right|^2 = \left|M(\alpha' \longrightarrow \beta')\right|^2 \qquad (\underline{\text{if}}\ T = T^+ e^{i\delta}) \tag{2.34}$$

This forbids transverse lepton or baryon polarization which could only occur because of a term $\sim \vec{s} \cdot (\vec{k} \times \vec{k}')$ which is odd under $\alpha, \beta \longrightarrow \alpha', \beta'$.

We shall now show that $T = T^+$ in the approximation $\alpha = 0$ both for the quasi-elastic process and for the case when all final states are summed over by using the unitarity relation to order G:

$$T_{weak} - T^+_{weak} = i T^+_{weak}\left(T_{strong} + \alpha T_{e.m.}\right) + i\left(T^+_{strong} + \alpha T^+_{e.m.}\right) T_{weak} \tag{2.35}$$

$$T = T_{strong} + \alpha T_{e.m.} + G T_{weak}.$$

For the quasi-elastic process $|\alpha\rangle = |\nu, \text{nucleon}\rangle$ and $|\beta\rangle = |\text{lepton}, \text{nucleon}\rangle$. T_{strong} gives zero acting on these states which are stable under strong interactions. Therefore $T^{+}_{weak} = T_{weak} + 0(\alpha)$ in this case and the theorem is proved.

Electromagnetic corrections will occur due to the diagram:

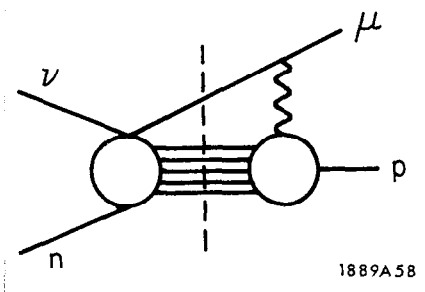

The leading correction ($\sim G^2 \alpha$) is due to the interference of this diagram and the usual first-order weak process. This involves the imaginary part of the amplitude in which the intermediate particles are on mass shell (indicated by the dashed line.) These corrections have been bounded in an interesting paper by De Rafael and de Rujula[D4] which we shall discuss in Section 3.3d.

When a complete set of final states $|\beta\rangle$ is summed over, the states may be taken to be eigenstates of the S matrix for strong interactions. The complete set of intermediate states inserted between T^{+} and T in Eq. (2.35) may also be taken to consist of eigenstates of S_{strong}. It follows from Eq. (2.35) that $T_{weak} = T^{+}_{weak} e^{i\delta} + 0(\alpha)$ in this case and the theorem is proved.

Note that the T violating structure function W_6 is bounded in terms of the others (Eq. 2.6 and 3.77). The inequalities require that $W_6 = 0$ in the deep inelastic region ($\nu \longrightarrow \infty$, ν/q^2 fixed) if either $\sigma_s = 0$ (Eq. 3.68) or the weak current is conserved.[D7] Both these conditions are expected to hold in the deep inelastic region according to currently fashionable theories (See section 3.6).

In other processes, transverse polarizations will only be forbidden by T invariance in the approximation that final state interactions are negligible (for a discussion see C9 and references therein). T invariance gives further restrictions for scattering from polarized targets but these do not seem worth discussing at present.

CHAPTER 3
PHENOMENOLOGICAL DESCRIPTIONS OF NEUTRINO REACTIONS

3.1. Neutrino Beams

We begin this chapter with a brief discussion of some experimental aspects of neutrino physics.* First we shall discuss neutrino beams of the type used at CERN and elsewhere, and then the monoenergetic neutrino beam which will be built at NAL.

At proton accelerators neutrino beams have usually been produced in the way which is schematically illustrated in Fig. 2. Important points to notice are:

1. Incident proton beams produce far more forward-going positive particles than negative particles (typically $\pi^+/\pi^- \sim$ 5-10/1). Therefore ν beams (from π^+ and K^+ decay) will be much more intense than $\bar{\nu}$ beams (from π^- and K^- decay)--see, e.g., Fig. 5. Furthermore the contamination of $\bar{\nu}$ beams by ν's (due to imperfect defocusing) will be much worse than the contamination of ν beams by $\bar{\nu}$'s. (The contamination must be accurately estimated in order to make tests of lepton conservation.)
2. The principal decay modes of π's and K's are $\pi \longrightarrow \mu + \nu_\mu$ and $K \longrightarrow \mu + \nu_\mu$. The beam therefore mainly consists of muon neutrinos. There are some ν_e's ($\bar{\nu}_e$'s) which come chiefly from the decays $K^\pm \longrightarrow \pi^0 e^\pm \nu_e (\bar{\nu}_e)$ and $\mu^\pm \longrightarrow e^\pm \nu_e (\nu_e) \bar{\nu}_\mu (\nu_\mu)$--see, e.g., Fig. 6. (It is important to estimate the $\nu_e (\bar{\nu}_e)$ background in order to test lepton conservation and measure or put limits on ν_e - e elastic scattering.)

---

*References to discussions of experimental techniques and developments at various laboratories may be traced from C7, C11, H3, and B36.

3. The energy of neutrinos from $\pi_{\mu 2}$ and $K_{\mu 2}$ decay is given by

$$E_\nu = \frac{M_\pi^2 - M_\mu^2}{2(E_\pi - p_\pi \cos\theta)} \approx \frac{E_\pi}{2} \text{ if } \theta = 0, \; E_\pi \gg M_\pi \quad (\pi \longrightarrow \mu\nu)$$

$$E_\nu = \frac{M_K^2 - M_\mu^2}{2(E_K - p_K \cos\theta)} \approx E_K \text{ if } \theta = 0, \; E_K \gg M_K \quad (K \longrightarrow \mu\nu) \tag{3.1}$$

where E_ν is the laboratory energy and θ the angle the neutrino makes with the parent meson's direction. It is therefore clear that the high energy part of the neutrino spectrum comes from K decay.

It may be possible in the future to "tag" the neutrinos in the broad spectrum neutrino beam described above.[H2] Otherwise the neutrino energy must be deduced by adding up the energy in the final state and a precise knowledge of the neutrino spectrum is necessary to interpret the results. Measurement of the spectrum usually proceeds in two ways:

1. The primary proton flux is continuously monitored. The flux of secondary pions and kaons is measured in a preliminary experiment (precise knowledge of the K/π ratio is essential since, as we shall see, there is a better way to measure the flux of ν's from π decay; alternative measurements of the ν flux from K decay are hard to perform). Using the known properties of the focusing system, the hadron flux in the decay tunnel, and hence the neutrino flux, can be calculated.
2. The muon flux from the decays $\pi/K \longrightarrow \mu\nu$ is measured thus providing a rather direct measurement of the ν flux. To this end detectors are placed in the shielding, the depth the muon penetrates giving its energy. There are two difficulties:

(a) Low energy μ's cannot be detected in this way since they only penetrate to small depths where the hadron flux is still appreciable.

(b) Only the $\pi \longrightarrow \mu\nu$ flux is well determined by this method. This is because the spectra of forward going μ's from π and K decay are similar (the maximum energy being approximately the energy of the parent in both cases) and the π/K ratio is so large. Because of the larger K mass, the angular distribution of μ's from K decay is broader than that of μ's from π decay. It may be possible to exploit this fact to monitor the $K \longrightarrow \mu\nu$ spectrum.

As a consequence of these facts the spectrum in the last CERN experiment was only well determined from about 1 - 4 GeV. Outside this range the first method was used ("renormalized" by the second) but it could not be considered very reliable since the K/π ratio was not well known.

It is obviously desirable to devise alternative methods of measuring the K flux. Other possibilities such as detecting γ's from the decays $K^{\pm} \longrightarrow \pi^{\pm}\ \pi^{o} \longrightarrow \pi^{\pm}\ \gamma\gamma$ perpendicular to the beam might be entertained but problems of neutron background probably make this impossible.

In Fig. 3 - 6 we show the broad band neutrino spectra anticipated in various beams of the type described above. A "monoenergetic" neutrino beam will be built at NAL,[C7] using an idea proposed some years ago[T3] (related designs were proposed earlier[P14]). A collimated π/K beam of well defined momentum is introduced into the decay tunnel. The target is designed and positioned to subtend a very small angle θ at the possible decay points. The spectrum is easily calculated using Eq. (3.1) and has the shape illustrated in Fig. 7.

Only a very rough measurement of the final state energy is necessary to distinguish neutrinos from the two energy bands. The flux can be measured by the

method already described. In the proposed beam, which is described in C7 (where details of the design, backgrounds from $K_{\ell 3}$ decays, etc., may be found), the two bands have energy spreads of ±6%, and it is calculated that the NAL machine running at 500 GeV can give $\sim 10^7$ ν's with energy 250 (±6%) GeV/pulse in this apparatus. Even if the gap between the bands turns out to be largely filled in, the results will still be much easier to interpret than those obtained with a conventional beam (however, the number of events will be much less). With the usual broad-band spectrum the flux falls roughly exponentially as a function of energy so that a small error in deducing the neutrino energy from the energy of the final state can lead to a large error in the cross section.

There is one other method of measuring the neutrino flux if we believe the conventional theory of weak interactions. In this case, neglecting the muon mass:

$$\left.\frac{d\sigma}{d|q^2|}\right|_{q^2=0}^{\nu n\to\mu^- p} = \left.\frac{d\sigma}{d|q^2|}\right|_{q^2=0}^{\bar{\nu} p\to\mu^+ n} = \frac{G^2\cos^2\theta_c}{2\pi}\left(1+\left|\frac{g_A}{g_V}\right|^2\right), \qquad (3.2)$$

which can be used to deduce the incident flux with hydrogen and, perhaps, deuterium targets. This method is not very reliable with nuclear targets since the cross section is strongly suppressed at small q^2 because of the Pauli principle (see Section 3.3) and this effect turns out to be very model-dependent. At large energies the quasi-elastic cross section is expected to be energy-independent (see Section 3.3) so that it can be used to determine the shape of the spectrum without knowledge of the form factors or the influence of the Pauli principle and the Fermi motion. However, this depends on being able to identify quasi-elastic events which is not easy with nuclear targets (due to reabsorption of produced π's, etc.)

Despite this, such a method was used in the early spark chamber experiments at CERN, following a suggestion by M. M. Block, and revealed that the flux was

about twice as large as originally thought. Block pointed out that there is a region ($0.1\ \mathrm{GeV}^2 \lesssim Q^2 \lesssim 0.2\ \mathrm{GeV}^2$) where Q^2 is large enough to escape the main effects of the exclusion principle yet small enough so that the result is insensitive to the axial form factor. Quasi-elastic events in this region, therefore, give the absolute flux if they can be identified with a nuclear target.

While on the subject of targets, we might remark that while counter experiments can use enormous targets and may be preferable for examining particular reactions, bubble chambers can more easily reveal possible surprises in high-energy neutrino reactions, such as violations of selection rules (but it may be necessary to employ them in conjunction with other devices to determine all the energy in the final state if a broad spectrum is used). In either case the advantages of using targets containing complex nucleii (better stopping power in bubble chambers as well as higher target mass) must be weighed against the difficulties of interpretation due to nuclear reabsorption and other effects at small q^2. It would be rash to dwell further on this subject in view of the many studies of experimental techniques now in progress.

3.2. Neutrino Lepton Interactions

The neutrino lepton interactions which are allowed in the usual theory and might be observed directly are

$$\nu_\mu + e^- \longrightarrow \mu^- + \nu_e \tag{3.3}$$

$$\nu_e + e^- \longrightarrow \nu_e + e^- \tag{3.4}$$

$$\bar{\nu}_e + e^- \longrightarrow \bar{\nu}_e + e^- \tag{3.5}$$

$$\bar{\nu}_e + e^- \longrightarrow \bar{\nu}_\mu + \mu^- \tag{3.6}$$

In addition, leptonic interactions can take place in the electromagnetic field of a target nucleus, e.g.:

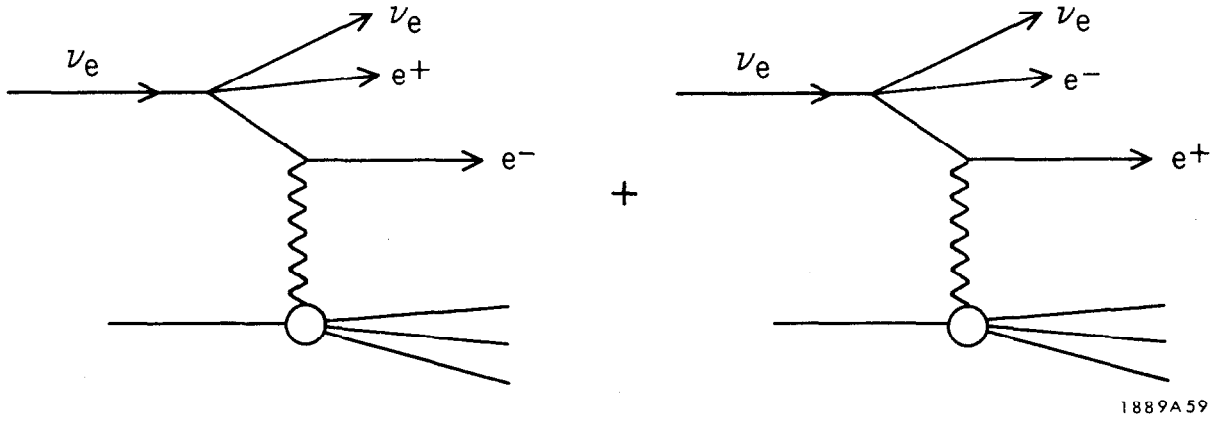

A. Interactions with electron targets

The existence of μ decay implies the existence of the processes (3.3) and (3.6). The limits for (3.4) and (3.5) were given on page 19 ; on the basis of the conventional theory, we shall conclude that there is little chance of measuring the cross sections for these processes directly in the near future. However, the conventional theory may be totally misleading at high energies.

An essential point is that even at NAL energies the center-of-mass energy is very low: $s = 2m_e E_\nu < 0.5\ \text{GeV}^2$, $S_{av.} \sim 0.01\ \text{GeV}^2$. Therefore, the cross sections are very small since dimensionally $\sigma \sim G^2 s$ and $G^2 S_{av.} \sim 10^{-39}\ \text{cm}^2$. In fact, assuming a 200-GeV proton beam, a target of 70 m^3 of liquid hydrogen (the hypothetical 25' chamber) and a "typical experiment" Nezrick calculated[N6]:

$\nu_\mu e^- \longrightarrow \mu^- \nu_e$	215 events
$\nu_e e^- \longrightarrow \nu_e e^-$	2.5 events
$\bar{\nu}_e e^- \longrightarrow \bar{\nu}_e e^-$	0.8 events
$\bar{\nu}_e e^- \longrightarrow \bar{\nu}_\mu \mu^-$	0.02 events

The low rates for $\nu_e / \bar{\nu}_e$ processes are due to the relatively feeble $\nu_e / \bar{\nu}_e$ flux. The reactions (3.4) and(3.5) will be hard to detect positively because of

background problems. For these reasons, we shall only discuss reaction (3.3) in detail here. Cross sections for the other processes are related as $s \longrightarrow \infty$ by:

$$\lim_{s\to\infty} \sigma\left(\nu_\mu e^- \longrightarrow \nu_e \mu^-\right) = \lim_{s\to\infty} \sigma\left(\nu_e e^- \longrightarrow \nu_e e^-\right)$$
$$= 3 \times \lim_{s\to\infty} \sigma\left(\bar{\nu}_e e^- \longrightarrow \bar{\nu}_\mu \mu^-\right) = 3 \times \lim_{s\to\infty} \sigma\left(\bar{\nu}_e e^- \longrightarrow \bar{\nu}_\mu \mu^-\right) \tag{3.7}$$

in the usual theory.

Let us examine the extra information which can be obtained by observing the reaction (3.3) which cannot be obtained from μ decay.[J4] Assuming a point interaction without derivative couplings we may write quite generally:

$$\mathcal{H} = \frac{1}{\sqrt{2}} \bar{\mu} \gamma_\lambda (1-\gamma_5)\, e\, \bar{\nu}_\mu \gamma_\lambda (g_V - g_A \gamma_5) \nu_e + h \cdot c + \mathcal{H}' \tag{3.8}$$

μ decay can be used to eliminate $\mathcal{H}'$, which contains e and μ in different combinations, but it obviously cannot determine g_A/g_V as long as the neutrinos are not observed.[J3] (The usual theory has $g_A/g_V = 1$, in which case (3.8) reduces immediately to the usual $\mathcal{H}_{eff}$ by a Fierz transformation provided $\mathcal{H}' = 0$.) Although the limits on $\mathcal{H}'$ are not very good, we shall assume $\mathcal{H}' = 0$. In this case[J4]:

$$\frac{d\sigma\left(\nu_\mu e^- \to \nu_e \mu^-\right)}{d\cos\theta} = \frac{\left(s - m_\mu^2\right)^2}{32\pi s^3} \left(|g_V|^2 + |g_A|^2\right)\left(A + B - \lambda (A - B)\right)$$
$$A = \left[\left(s + m_e^2\right) - \left(s - m_e^2\right)\cos\theta\right]\left[\left(s + m_\mu^2\right) - \left(s - m_\mu^2\right)\cos\theta\right]$$
$$B = 4s^2 \tag{3.9}$$
$$\lambda = + \frac{2\,\mathrm{Re}\left(g_V^* g_A\right)}{|g_V|^2 + |g_A|^2} \quad (= 1 \text{ in the conventional theory})$$

where θ is the angle between the incident ν_μ and the μ^- in the center of mass. The θ distribution clearly determines λ, the most striking λ dependence being

$$\frac{d\sigma(\theta = 0)}{d\sigma(\theta = \pi)} \xrightarrow{s \gg m_e^2} \frac{1}{2}(1 + \lambda) \tag{3.10}$$

a result which can be derived directly from the fact that the μe vertex conserves helicity as $s \to \infty$. If a few hundred events are obtained at NAL, it will be possible to determine λ approximately.

B. Interactions in the electromagnetic field of a nucleus

The cross sections for these processes can be calculated exactly to order $G^2\alpha^2$ in terms of known quantities if $\mathscr{L}_{\text{eff}}$ is assumed for leptonic interactions (the existence of an IVB would only alter the results by adding terms of order M_μ^2/M_W^2). The dominant process is that in which the nucleus (of charge Ze) recoils coherently. The first detailed calculations were done by Czyz, Sheppey and Walecka[C28] (approximate results having been obtained previously[B14,K2,K12,S5]) who found:

$$\sigma\left(\nu_\mu Z \to \mu^- e^+ \nu_e Z\right) \xrightarrow[E \to \infty]{} \frac{5Z^2\alpha^2G^2}{72\pi^2} E_\nu \beta \left\{ \ell n\left(\frac{2E_\nu}{\beta}\right) + \frac{1}{3}\ell n\left(\frac{2E_\nu\beta}{m_\mu^2}\right) - \frac{193}{90} - \frac{\beta^2}{150\, m_\mu^2} \right\} \tag{3.11}$$

$$\sigma\left(\nu_\mu Z \to \mu^- \mu^+ \nu_\mu Z\right) \xrightarrow[E \to \infty]{} \frac{5Z^2\alpha^2G^2}{72\pi^2} E_\nu \beta \left\{ \frac{4}{3}\ell n\left(\frac{2E_\nu\beta}{m_\mu^2}\right) - \frac{332}{45} - \frac{2\beta^2}{75\, m_\mu^2} \right\} \tag{3.12}$$

using a nuclear form factor

$$F\left(q^2\right) = \frac{1}{\left(1 - q^2/\beta^2\right)^2} \qquad \beta = \frac{\sqrt{20}}{R_0} = 1.2\, A^{1/3} \text{ fm} .$$

Results obtained with an exponential form factor are also given in C28 as are the cross sections for processes with incident ν_e's (neither choice of form factor gives a good fit to the observed charge distribution--see, e.g., Fig. 3 of L24--the two forms were supposed to bracket the actual behavior as $Q^2 \to \infty$). The asymptotic formulae (3.11) and (3.12) are compared with the exact cross section in Fig. 8. Cross sections for various nuclei are given in Fig. 9.

In order to distinguish these four fermion events from other processes which yield a muon pair ($\nu_\mu \mathrm{Pb} \to \mu^- \pi^+ (\to \mu^+ \nu) + \ldots$, $\nu_\mu \mathrm{Pb} \to \mu^- W^+ (\to \mu^+ \nu) + \ldots$) the distributions in the muon variables must be calculated. This has been done by Fujikawa[F13] (whose results are quoted in H3) and by Løvseth and Radomski.[L24] These calculations are of interest in their own right since the results can eventually be confronted with experiment. At present the most important results concern the experimental signature of the four fermion processes.

Unfortunately it is the author's impression that Fujikawa's results disagree with those of Løvseth and Radomski (compare, e.g., Fig. 6 of L24 with Fig. 16 of F13) but it is hard to pin this down since, except in a few cases, they plot different distributions. There is agreement that the μ^- tends to continue in the direction of the ν and take most of its energy. However, in Ref. H3 it is claimed, on the basis of Fujikawa's calculations, that the muons have transverse momentum 0 - 50 MeV (see Table 3). In contrast Løvseth and Radomski find (e.g.) for $\nu_\mu \mathrm{Pb} \to \nu_\mu \mu^+ \mu^- \mathrm{Pb}$ that $\langle P^{t3}_{\mu^+} \rangle \simeq \langle P^{t3}_{\mu^-} \rangle \simeq 70$ MeV at $E_\nu = 1.5$ GeV increasing to $\langle P^{t3}_{\mu^+} \rangle \simeq 200$ MeV and $\langle P^{t3}_{\mu^-} \rangle \simeq 290$ MeV at $E_\nu = 40$ GeV (their quantity P^{t3} is almost the transverse momentum at small angles). This apparent discrepancy is very serious since the ability to distinguish the four fermion processes from other reactions in the experiment to be performed at NAL[H3] hinges on the characteristics of the transverse momentum distributions. The authors of this NAL proposal give the estimates in Table 3 , on the basis of which they conclude that the four fermion cross sections can be measured to ±10% in 30 - 60 days running time. Løvseth and Radomski using their larger value of the transverse momentum are less optimistic. In view of this apparent disagreement, we do not quote detailed results here. It is comforting that a third independent calculation is under way.[S11]

3.3. Quasi-elastic Neutrino Scattering ($\Delta Y = 0$)

A. General Remarks

The hadronic current describing the process

$$\nu(k_1) + n(p_1) \longrightarrow \ell^-(k_2) + p(p_2)$$

may be written

$$\langle p(p_2) \left| J_\lambda^+ \right| n(p_1) \rangle = \cos\theta_c\, \bar{u}(p_2)\, \Gamma_\lambda\, u(p_2)$$

$$\Gamma_\lambda = \gamma_\lambda F_V^1(q^2) + \frac{i\sigma_{\lambda\nu}\, q^\nu\, \xi\, F_V^2(q^2)}{2M} + \frac{q_\lambda F_V^3(q^2)}{M}$$

$$+ \gamma_\lambda\gamma_5 F_A(q^2) + \frac{q_\lambda \gamma_5 F_p(q^2)}{M} + \frac{\gamma_5 (p_1+p_2)_\lambda F_A^3(q^2)}{M} \qquad (3.13)$$

$$= \gamma_\lambda \left(F_V^1 + \frac{(M_1+M_2)\,\xi F_V^2}{2M} \right) + \frac{q_\lambda F_V^3}{M} - \frac{(p_1+p_2)_\lambda\, \xi F_V^2}{2M}$$

$$+ \gamma_\lambda\gamma_5 \left(F_A + \frac{(M_2-M_1)\, F_A^3}{M} \right) + i\gamma_5 \frac{\sigma_{\lambda\nu}\, q^\nu\, F_A^3}{M} + \frac{q_\lambda \gamma_5 F_p}{M}$$

$$\left(q = k_1 - k_2 = p_1 - p_2\,,\quad M = \frac{M_1+M_2}{2} \right)$$

The relation to the form factors used by some other authors is given in the appendix (we keep $M_1 \neq M_2$ for convenience in going to the $\Delta Y \neq 0$ case and introduce $\xi = \mu_p - \mu_n$ so that $F_V^2(0) = 1$ if the isotriplet current hypothesis is correct). Experimental results for β decay at $q^2 \simeq 0$ agree with Eq. (3.15) below within the errors and give $F_A(0) = -1.23 \pm 0.01$.

For the process:

$$\bar{\nu}(k_1) + p(p_1) \longrightarrow \ell^+(k_2) + n(p_2)$$

the current is

$$\langle n(p_2)\left|J_\lambda^-\right|p(p_1)\rangle = \cos\theta_c \bar{u}(p_2)\,\tilde{\Gamma}_\lambda\, u(p_1) = \langle p(p_1)\left|J_\lambda^+\right|n(p_2)\rangle^*$$

(3.14)

$$\tilde{\Gamma}_\lambda(p_1, p_2) = \gamma_0\,\Gamma_\lambda^+(p_2, p_1)\,\gamma_0$$

The various hypotheses about J_λ discussed in Chapter 1 restrict the form factors as follows:

(1) T invariance $\longrightarrow$ All form factors real (apart from an arbitrary overall phase factor which we take to be real henceforth).

(2) Charge symmetry $\longrightarrow$ $F_V^{1,2}$, F_A and F_P real. $F_{V,A}^3$ imaginary.

(3) No second-class currents $\longrightarrow$ $F_{V,A}^3 = 0$ ($\equiv$ T invariance + charge symmetry).

(4) CVC $\longrightarrow$ $F_V^3 = 0$.

(5) Isotriplet current

$$F_V^1(q^2) = \left[F_1^p(q^2) - F_1^n(q^2)\right] = \text{Dirac electromagnetic isovector form factor.}$$

(3.15)

$\xi = \mu_p - \mu_n = 3.71$ (μ = anomalous magnetic moment)

$$F_V^2(q^2) = \frac{\mu_p F_2^p(q^2) - \mu_n F_2^n(q^2)}{\mu_p - \mu_n} = \text{Pauli electromagnetic isovector form factor.}$$

In terms of the Sachs form factors

$$F_V^1(q^2) = \left(1 - \frac{q^2}{4M^2}\right)^{-1}\left[G_E^V(q^2) - \frac{q^2}{4M^2}\,G_M^V(q^2)\right]$$

(3.16)

$$\xi F_V^2(q^2) = \left(1 - \frac{q^2}{4M^2}\right)^{-1}\left[G_M^V(q^2) - G_E^V(q^2)\right]$$

Experimentally, the G's are described to within ± 10% by:

$$G_E^V(q^2) = \frac{1}{\left(1 - \frac{q^2}{0.71\ \text{GeV}^2}\right)^2}$$

$$G_M^V(q^2) = \frac{1+\mu_p - \mu_n}{\left(1 - \frac{q^2}{0.71\ \text{GeV}^2}\right)^2} \qquad (3.17)$$

Important points to notice about the quasi-elastic process are:

(1) If polarizations are not measured, only 3 combinations of the 6 complex form factors can be determined according to the general theorems in Section 2.1. We have

$$\frac{d\sigma}{d|q^2|}\left(\begin{matrix}\nu\, n\to\ell^-\, p\\ \bar\nu\, p\to\ell^+\, n\end{matrix}\right) = \frac{M^2G^2\cos^2\theta_c}{8\pi E_\nu^2}\left[A(q^2)\mp B(q^2)\frac{(s-u)}{M^2} + \frac{C(q^2)(s-u)^2}{M^4}\right] \qquad (3.18)$$

$$(s-u = 4ME_\nu - q^2 - m^2)$$

The relation between ν and $\bar\nu$ experiments follows from Eq. (2.8) and (2.11). To derive this relation directly[B6], note that if electromagnetic corrections are neglected $T = T^+$ for these processes (see Chapter 2.3) so that

$$\sum_{\text{spins}} \left|M_{\nu\, n\to\ell^-\, p}\right|^2 = \sum_{\text{spins}} \left|M_{\ell^-\, p\to\nu\, n}\right|^2 \qquad (3.19)$$

Because of CPT invariance, the spin averaged lepton tensors (2.3) satisfy:

$$m_{\mu\nu}\left(\ell^-(k_2)\to\nu(k_1)\right) = m_{\mu\nu}\left(\bar\nu(k_1)\to\ell^+(k_2)\right)\left[= m_{\mu\nu}\left(\bar\nu(-k_1)\to\ell^+(-k_2)\right)\right]. \qquad (3.20)$$

Hence

$$\begin{matrix} d\sigma(s,t,u) & = & d\sigma(u,t,s)\\ \nu\, n\to\ell^-\, p & & \bar\nu\, p\to\ell^+\, n\end{matrix} \qquad (3.21)$$

In terms of the form factors in (3.13) (putting $M_1 = M_2$ now) the functions A, B and C (3.18) are given explicitly by (see, e.g., M4, P4 or A2):

$$A = \frac{(m^2 - q^2)}{4M^2}\left[\left(4 - \frac{q^2}{M^2}\right)\left|F_A\right|^2 - \left(4 + \frac{q^2}{M^2}\right)\left|F_V^2\right|^2 - \frac{q^2}{M^2}\left|\xi F_V^2\right|^2\left(1 + \frac{q^2}{4M^2}\right)\right.$$

$$- \frac{4q^2\,\mathrm{Re}\,F_V^{1*}\xi F_V^2}{M^2} + \frac{q^2}{M^2}\left(4 - \frac{q^2}{M^2}\right)\left|F_A^3\right|^2$$

$$\left. - \frac{m^2}{M^2}\left(\left|F_V^1\right|^2 + \left|F_A + 2F_P\right|^2 + \left(\frac{q^2}{M^2} - 4\right)\left(\left|F_V^3\right|^2 + \left|F_P\right|^2\right)\right)\right] \qquad (3.22)$$

$$B = + \frac{q^2}{M^2}\,\mathrm{Re}\,F_A^*\left(F_V^1 + \xi F_V^2\right) + \frac{m^2}{M^2}\,\mathrm{Re}\left[\left(F_V^1 + \frac{q^2}{4M^2}\,\xi F_V^2\right)^* F_V^3 - \left(F_A + \frac{q^2 F_P}{2M^2}\right)^* F_A^3\right]$$

$$C = \frac{1}{4}\left(\left|F_A\right|^2 + \left|F_V^1\right|^2 - \frac{q^2}{M^2}\left|\frac{\xi F_V^2}{2}\right|^2 - \frac{q^2}{M^2}\left|F_A^3\right|^2\right)$$

(2) Unless some of the form factors behave very differently from the others, A, B and C (3.18) will be of the same order of magnitude. Since A, B and C presumably fall off rapidly with Q^2, only C is measured as $s \to \infty$. To obtain the maximum information neutrinos of $\sim$ 1 GeV are required.

(3) The contributions of the form factors F_P and $F_V^3 \sim m^2$ $\left(J_\lambda \sim q_\lambda F_P/F_V^3;\ q_\lambda j^\lambda \sim m\right)$ and are therefore hard to detect unless these form factors are unexpectedly large.

(4) In the approximation m = 0 the only contribution of second-class currents $\sim \left|F_A^3\right|^2$. The absence of interference terms between the two classes of currents means that it would be hard to detect second-class currents with small form factors.

B. Cross Sections in the Conventional Theory and Theoretical Ideas about the Axial Form Factors

In the conventional theory, in which the hypotheses listed on page 58 are satisfied, there are two unknown form factors in elastic neutrino scattering: F_A and F_P. F_A can be determined rather directly by measuring $d\sigma^{\nu} - d\sigma^{\bar{\nu}}$ which, because of the assumption of charge symmetry (page 39), depends only on the V-A interference term:

$$\frac{d\sigma^{\nu n \to \ell^- p}}{d|q^2|} - \frac{d\sigma^{\bar{\nu} p \to \ell^+ n}}{d|q^2|} = \frac{G^2 \cos\theta_c}{4\pi M^2 E_\nu^2} (s-u) q^2 F_A^* G_M^V \qquad (3.23)$$

Up to now extensive $\bar{\nu}$ experiments have not been performed, nor are the ν experiments nearly accurate enough to allow $F_A(q^2)$ and $F_P(q^2)$ to be determined. The usual procedure is to assume the functional form

$$F_A(q^2) = -1.23 \Big/ \left(1 - \frac{q^2}{M_A^2}\right)^n \qquad (3.24)$$

and to use a model for F_P or neglect its contribution ($\sim m^2$). The results of model calculations with $n = 2$ are shown in Fig. 10 - 13 (cross sections are given in M4 for a wide range of form factors).

Experiments have not even been able to determine the best value of n up to now but $n = 2$ is usually assumed by analogy to the electromagnetic case. This is very unsatisfactory. The remarkable scaling law $G_E(q^2)/G_M(q^2) \simeq$ const. suggests that G_E and G_M describe the same distribution of "stuff" inside the nucleon and we might therefore be tempted to assume that the axial form factor is similar. In the absence of a dynamical understanding of the scaling law, however, we have no criterion to decide which combination (if any) of the axial form factors should

behave like G_E and G_M (an unusual choice of form factors which has some advantages has been discussed by Ketley).[K7] On the other hand, the experimental discovery of such a combination might shed light on the scaling law.

There is one piece of evidence in favor of taking n = 2 in Eq. (3.24). $F_A(q^2)$ can be calculated in terms of single pion electroproduction data near threshold using PCAC and current algebra. The results of one calculation rule out n = 1 and give $M_A = 1.34 \pm 0.05$ GeV with n = 2.[N5] However, other authors (e.g. F15) find different results. The data is probably not good enough to make a reliable determination of F_A by this method at present. (When the processes $ep \longrightarrow ep\,\pi^o$ and $ep \longrightarrow en\,\pi^+$ have been separated it will be possible to check the reliability of the method by using it to calculate a combination of the known form factors G_M and G_E.)

Near $q^2 = 0$ we expect F_P to be dominated by the pion pole:

$$\frac{F_p(q^2)}{M} \simeq \frac{\sqrt{2}\, g_{NN\pi} f_\pi}{q^2 - M_\pi^2} \quad , \quad (q^2 \simeq 0) \, . \tag{3.25}$$

PCAC gives

$$F_p(q^2) \simeq \frac{2M^2 F_A(0)}{q^2} \left[\frac{1}{1 - q^2/M_\pi^2} - \frac{F_A(q^2)}{F_A(0)} \right], (q^2 \simeq 0) \tag{3.26}$$

which agrees with Eq. (3.25) provided

$$\left| \frac{1}{F_A(0)} \left. \frac{\partial F_A}{\partial q^2} \right|_{q^2 = 0} \right| \ll \frac{1}{M_\pi^2} \, ,$$

which is presumably the case. According to these formulae $F_P(q^2)$ is much larger than $F_A(q^2)$ near $q^2 = 0$ and this is borne out by experiments on μ capture. There is no reason to believe Eq. (3.25) or (3.26) away from $q^2 \simeq 0$. However, if we believed that the axial current would be conserved if M_π were zero, then $F_p(q^2) = (2M^2 F_A(q^2))/(M_\pi^2 - q^2)$ might be a reasonable approximation for all q^2.

Some authors have normalized $F_p(q^2)$ to $-\sqrt{2}\, g_{NN\pi} f_\pi / M_\pi^2$ at $q^2 = 0$ and given it the same q^2 dependence as F_v^1 or G_E^v for $q^2 < 0$. This implies an abrupt change of behavior at $q^2 = 0$. With $F_p \propto F_v^1$ (e.g.) it gives

$$\left.\frac{\partial F_p}{\partial Q^2}\right|_{q^2=-\epsilon} = -\frac{F_p(0)}{0.71\ \mathrm{GeV}^2}$$

while the assumption that the pion pole dominates in $0 < q^2 < M_\pi^2$, which is implicit in this choice of normalization, yields

$$\left.\frac{\partial F_p}{\partial Q^2}\right|_{q^2=+\epsilon} = -\frac{F_p(0)}{M_\pi^2} \quad .$$

This procedure of normalizing near the pole certainly overestimates F_p for small Q^2 (the contribution of F_p to the cross section from large Q^2 is negligible if F_p falls off like $1/Q^2$ or faster as $Q^2 \to \infty$).

With this dubious choice of q^2 dependence F_p can make a substantial contribution to the cross section, although it enters multiplied by $\frac{m}{M}$, because $F_p(0) \simeq -90 F_A(0)$. Thus with $F_p(q^2) = F_p(0) F_v^1(q^2)$ Yamaguchi found[Y2] that it contributed $\sim 20\%$ to the cross section for $E_\nu \sim M$, although its contribution was negligible for $E_\nu \gg M$ and $E_\nu \ll M$. We believe that this is like to be a gross exaggeration of the effect of F_p.

We conclude that the contribution of F_P is probably not more than a few percent. In the absence of more compelling theoretical arguments it is probably best to ignore F_P until the experiments are accurate enough to check any model or parameterization adopted for it.

The results expected from a ν or $\bar{\nu}$ experiment at Argonne are shown in Table 4 where the errors expected in the determination of various parameters

are shown. The ν experiment can measure M_A (Eq. 3.24) but it is very insensitive if other parameters are allowed to vary. The $\bar{\nu}$ experiment is able to determine M_A and any large derivations from CVC, although there are many fewer events. However, if a good fit cannot be achieved with CVC, it would perhaps be more natural to keep CVC but abandon the assumption $F_A^3 = 0$.

C. Polarization Measurements

The quasi-elastic cross section when both the final lepton and baryon polarizations are measured has been given by Adler[A2] for $\Delta Y = 0$ and $\Delta Y = \pm 1$ reactions (see also E2, K7 and P4--the relation between our form factors and those used by these authors is given in the appendix). Here we will make some simplifying assumption and try to pick out the leading terms.

In the approximation m = 0 the lepton vertex conserves helicity. Interesting lepton polarization effects are therefore proportional to m and hard to measure. The polarizations may be obtained directly from Eq. (2.12) using

$$W_i = 2\delta\left(2\nu + q^2\right)\omega_i$$

$$\omega_1' = \omega_1 = \left|F_A\right|^2 - \frac{q^2}{4M^2}\left(\left|F_A\right|^2 + \left|F_V' + \xi F_V^2\right|^2\right)$$

$$\omega_2' = \omega_2 = \left|F_A\right|^2 + \left|F_V'\right|^2 - \frac{q^2}{M^2}\left(\left|\frac{\xi F_V^2}{2}\right|^2 + \left|F_A^3\right|^2\right)$$

$$\omega_3' = \omega_3 = 2\,\mathrm{Re}\; F_A^*\, F_V'$$

$$\omega_4' = 4\omega_4 + \omega_2 - 2\omega_5 = -\left|F_V'\right|^2 - \left|F_A + 2F_P\right|^2 + \left(4 - \frac{q^2}{M^2}\right)\left(\left|F_V^3\right|^2 + \left|F_P\right|^2\right) \qquad (3.27)$$

$$\left.\begin{aligned}\omega_5' &= \omega_5 - \omega_2 = \mathrm{Re}\\ \omega_6' &= \omega_6 = \mathrm{Im}\end{aligned}\right\} 2\left[\left(F_V' + \frac{q^2\,\xi F_V^2}{2M^2}\right)^* F_V^3 - \left(F_A + \frac{q^2 F_P}{2M^2}\right)^* F_A^3\right]$$

The ω_i' occur naturally if the hadron tensor $W_{\mu\nu}$ is expanded in terms of $p + p'$ and q rather than p and q. They are much more convenient than the ω_i for many purposes in the quasi-elastic case.*

The unpolarized cross section essentially determines $\omega_{1,2,3}$ (dropping terms of order m^2). Polarization effects are, therefore, only of interest insofar as they contain information about $\omega_{4,5,6}$. Note that the contributions of $\omega_{4,5,6}$ vanish as $q^2 \longrightarrow 0$ ($\theta \longrightarrow 0$). Since most of the events presumably occur at small q^2, it will therefore be hard to obtain useful information from lepton polarization measurements. The deviation of the longitudinal lepton (antilepton) polarization from -1 (+1) is hardly amenable to measurement being of order m^2 (unless the V-A lepton current gives an incorrect description at high energies). The perpendicular polarization is proportional to $m \sin\theta$ but we note that the extra structure function which it determines (ω_5) enters multiplied by E' and, unfortunately, as θ and Q^2 increase,

---

*E.g., in terms of the ω_i' the coefficients A, B and C (Eq. 3.18 and 3.22) have the simple form[P4]:

$$4M^2 A = \left(m^2 - q^2\right)\left(8M^2\omega_1' - \left(4M^2 - q^2\right)\omega_2' + m^2\omega_4'\right)$$

$$2M^2 B = -q^2\omega_3' \pm m^2\omega_5'$$

$$4C = \omega_2'$$

Note that $\omega_i'^{\,\nu n\to\mu^- p} = \omega_i'^{\,\bar{\nu} p\to\mu^+ n}$ $\quad (i \neq 5)$

$$\omega_5'^{\,\nu n\to\mu^- p} = -\omega_5'^{\,\bar{\nu} p\to\mu^+ n}$$

ω_5' vanishes if there are no second-class currents.

E' decreases. We conclude that longitudinal and perpendicular lepton polarizations are not very useful tools in practice. We will discuss the transverse polarization in the next section.

It is hard to measure the baryon polarization unless the apparatus is designed with that purpose in mind. Jovanic and Block[J6] have considered surrounding a deuterium target with Aℓ spark chambers; the transverse and perpendicular polarizations are measured when the nucleon rescatters from the Aℓ plates. Alternatively this could be achieved by inserting Aℓ plates in a bubble chamber. This might be worth while at NAL energies at which the unpolarized quasi-elastic cross section depends only on $C(q^2)$ in Eq. (3.22) which contains little information on its own. We shall see below that the polarizations depend on quite different combinations of form factors than $C(q^2)$.

Before giving detailed formulae we consider some general properties. When $\theta_{\mu\nu} = \pi \left(Q^2 = Q^2_{max} = 4ME^2/(M+2E) + 0(m^2) \right)$ it follows from angular momentum conservation that in the approximation $m = 0$ the final baryon is 100% longitudinally polarized (with negative helicity in the center of mass and laboratory) because the conventional lepton vertex conserves helicity. As $\theta_{\mu\nu} \longrightarrow 0 \left(Q^2 \longrightarrow 0(m^2) \right)$ angular momentum conservation requires that in the center of mass the transverse and perpendicular polarizations vanish; the longitudinal polarization is, of course, known and is almost 100% (with negative helicity) because $g_A/g_V \approx -1$ (this polarization is completely perpendicular in the laboratory because $\vec{q} = \vec{p}'$ is essentially perpendicular to $\vec{k}$ for infinitesimal Q^2). Interesting polarization effects, therefore, occur at intermediate Q^2.

In the conventional theory the cross section when the final baryon is perpendicularly polarized may be written[B32]:

$$\frac{d\sigma^{\uparrow x}}{d|q^2|} - \frac{d\sigma^{\downarrow x}}{d|q^2|} = \frac{G^2 \cos^2\theta_c \sin\phi_p}{2\pi} \left\{ -2 F_A F_v' - \frac{-q^2}{2M^2} \left[F_A \xi F_v^2 \right.\right. \tag{3.28}$$

$$\left.\left. + \frac{M}{E} F_v' \left(F_v' + \xi F_v^2 + F_A \right) \right] + \frac{q^4}{16 M^2} \frac{M}{E} \left(\left| \xi F_v^2 \right|^2 + \xi F_v^2 \left(F_v' + F_A \right) \right) \right\}$$

$$\left(\sin\phi_p = \sqrt{\frac{4M^2E^2 + q^2(M^2 + 2ME)}{(4M^2 - q^2)E^2}} + 0\left(\frac{m^2}{E^2}\right) \right)$$

where $\uparrow x$ ($\downarrow^x$) indicates laboratory polarization $\parallel$ (anti $\parallel$) to x defined by:

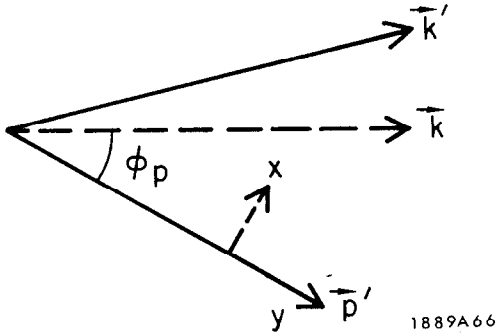

Equation (3.28) provides another way to determine F_A. If this were inconsistent with the result obtained from the differential cross section, we would have to turn to the general case with all form factors retained which is given, e.g., in A2 and P4. Here we give only the limit of the polarization as $E \longrightarrow \infty$ with Q^2 fixed, which is the interesting part for experiments at NAL:

$$P^x(\text{perp}) = -\sqrt{\frac{4M^2}{4M^2 - q^2}} \frac{\left[2\,\text{Re}\left(F_v^1 + \frac{q^2}{4M^2} \xi F_v^2 \right)^* F_A - \frac{q^2}{M^2} \text{Re}\left(F_v^1 + \xi F_v^2 \right)^* F_A^3 \right]}{|F_A|^2 + |F_v'|^2 - \frac{q^2}{4M^2} |\xi F_v^2|^2 - \frac{q^2}{M^2} |F_A^3|^2} + 0\left(\frac{1}{E}\right). \tag{3.29}$$

Longitudinal polarization cannot be measured by rescattering the baryon. It is therefore inaccessible unless the apparatus is in a magnetic field so that the

direction of the polarization is different at the production point and the point of rescattering. Here we give the leading terms in the general case as $E \longrightarrow \infty$, with Q^2 fixed:

$$P^y(\text{long}) = 2\sqrt{\frac{-q^2}{4M^2-q^2}}\ \frac{\mathrm{Re}\left(2F_v' + \frac{q^2\xi F_v^2}{2M^2}\right)^* F_A^3 - \mathrm{Re}\left(F_v' + \xi F_v^2\right)^* F_A}{|F_A|^2 + |F_v'|^2 - \frac{q^2}{4M^2}|\xi F_v^2|^2 - \frac{q^2}{M^2}|F_A^3|^2} + 0\left(\frac{1}{E}\right) \qquad (3.30)$$

The polarizations with incident autineutrinos are given, e.g., in (A2) and (P4) (they can be deduced from Eq. (3.42) and (3.43) below in the conventional theory). The general arguments above still apply except that the helicity is now positive when $\theta_{\mu\nu} = \pi$, in the approximation m = 0. The results of a model calculation with incident autineutrinos are shown in Fig. 25 and 26.

D. T Violating Effects

In Section 2.3 we discussed the fact that, in the absence of electromagnetic corrections, transverse polarizations (out of the reaction plane) would indicate T violation. The transverse lepton polarization is given by Eq. (3.27) and (2.12). The cross section when the final baryon is polarized along $\vec{S}_{trans} \sim \vec{k} \times \vec{k}'$ is given by[A2,P4]:

$$\left(\frac{d\sigma(+S_{trans})}{d|q^2|} - \frac{d\sigma(-S_{trans})}{d|q^2|} \right)_{\substack{\text{final} \\ \text{baryon} \\ \text{polarized}}} = \frac{G^2 \sqrt{-q^2(4M^2E^2+q^2)+q^2(2ME+M^2)}}{8\pi M^3 E^2}$$

$$\times \text{ Im} \left[(4ME+q^2) \left(\left[F_v' + \xi F_v^2 \right]^* \frac{\xi F_v^2}{2} - F_A^* F_A^3 \right) + 2M^2 F_A^* \left(F_v' + \frac{q^2 \xi F_v^2}{4M^2} \right) \right.$$

$$\left. + q^2 F_A^{3*} \left(F_v' + \xi F_v^2 \right) \right] \qquad (3.31)$$

These effects can be estimated[B15,F12] in the theory of T violation due to Cabibbo[C2] who introduced second-class currents with form factors comparable to the first-class form factors but 90^o out of phase (second-class currents must be introduced if we wish to have T violation without abandoning the charge symmetry condition). Using the limit on F_v^3 from μ capture it turns out that it gives a very small contribution[B15] and we shall ignore it (unless we abandon CVC, $F_v^3 = 0$ in any case). Results obtained with $F_A^3 = i\left(\xi F_v^2/2\right)$ and the conventional dipole fit for the other form factors are shown in Fig. 14c. The baryon polarization is insensitive to F_p. However, the muon polarization is proportional to the divergence of the axial current (W_6 vanishes if $\partial_\mu A_\mu = 0$) and this is sensitive to the choice of F_p. The results in Fig. 14 were obtained using Eq. (3.26). Berman

and Veltman[B15] obtained much larger results following essentially the same prescription as Yamaguchi which probably greatly exaggerates F_p, as we argued in Section 3.3B.

If substantial transverse polarization is found, sceptics might attribute it to electromagnetic corrections (although we would expect them to be of order α). This loophole has been closed for baryon polarizations of the magnitude given by taking $F_A^3 = i\left(\xi F_V^2/2\right)$, however, by De Rafael and de Rujula[D4] who have bounded the electromagnetic effects which simulate T violation by using the Schwartz inequality to bound the contribution of each half of the diagram on page 46 in terms of known data. The bound is shown in Fig. 14; it is presumably comfortably satisfied since much information is lost in the use of the Schwartz inequality.

E. Nuclear Effects

Up to now all neutrino experiments have used complex nuclei as targets. This complicates the analysis since the nuclear effects turn out to be quite model dependent. Eventually the quasi-elastic form factors will be accurately measured by experiments on hydrogen and deuterium (we return to the nuclear effects in the latter case at the end of this section) and the experiments on nuclei will give interesting information about nuclear structure.

Even to speak of quasi-elastic neutrino scattering on nucleons bound in nuclei is to picture the nucleus as a collection of almost free nucleons and we shall neglect many body terms, off-mass shell effects, etc. The most important nuclear effects are due to

1. The Fermi motion
2. The Pauli principle
3. Rescattering and absorption of recoiling hadrons

The last effect obscures the interpretation because it allows processes such as $\nu N \longrightarrow \mu N \pi$ to be mistaken for the quasi-elastic process when the pion is re-absorbed. This effect is discussed in (L23) and (B45). The Fermi motion spreads out the quasi-elastic peak in $q^2-\nu$ space. We neglect it here referring to (L23, L22, Y5) for discussion and references.

The most important nuclear effect is due to the Pauli principle. In a simple Fermi gas model the quasi-elastic process is only allowed if the momentum of the recoiling proton (neutron) lies outside the Fermi sphere of protons (neutrons) present initially. A simple calculation gives the result that in this model the cross section per neutron is equal to the cross section on a free neutron multiplied by[G2, B14]

$$1 - N^{-1} D \tag{3.32}$$

where

$$\begin{aligned} D &= Z && \text{for } 2x < u-v \\ &= \frac{1}{2}A\left\{1 - \frac{3x}{4}\left(u^2+v^2\right) + \frac{x^3}{3} - \frac{3}{32x}\left(u^2-v^2\right)^2\right\} && \text{for } u-v < x < u+v \\ &= 0 && \text{for } x > u+v \end{aligned} \tag{3.33}$$

$$x = \frac{|\vec{q}|}{2k_f}\ , \qquad u = \left(\frac{2N}{A}\right)^{1/3}\ , \qquad v = \left(\frac{2Z}{A}\right)^{1/3}$$

(N, Z, A) = (neutron, proton, nucleon) number

k_F is the Fermi momentum and $|\vec{q}| = \sqrt{(q^2+m^2)/4M^2 - q^2}$ is the three-momentum transfer to a stationary target neutron (the same formula holds for the process $\bar{\nu}p \longrightarrow \mu^+ n$ with $N \longleftrightarrow Z$). The function $1 - N^{-1} D$ is plotted in Fig. 15 and 16 for two cases.

We have recently carried out extensive calculations using shell model wave functions and the kinematics which would obtain if the target were a single stationary

nucleon[B11] (this paper contains many references to previous work on this subject and on the related problem of μ capture). In this approach spin is important and it is necessary to distinguish three exclusion factors:

$$D_{S,T,L} = -\left(\psi \left| \sum_{n \neq m} e^{i\vec{q}\cdot\left(\vec{x}_n - \vec{x}_m\right)} \tau_n^- \tau_m^+ \left(1, \sigma_{xn}\sigma_{xm}, \sigma_{zn}\sigma_{zm}\right) \right| \psi \right) \qquad (3.34)$$

where $\vec{x}_n$ are the coordinates of the nucleons, σ_{xn} the x component of the spin operator for the n^{th} nucleon, $\tau_n^{\pm}$ the isospin raising (lowering) operators, ψ the ground state wave function and $\vec{q}$ is taken to be along the z axis. The cross section per neutron in the conventional theory in the approximation m = 0 is given by

$$\frac{d\sigma}{d\Omega} = \frac{1}{64\pi^2 M^2}\left(\frac{E'}{E}\right)^2 \left(|\alpha|^2 \left(1 - N^{-1} D_S\right) + \left(|\beta x|^2 + |\beta y|^2\right)\left(1 - N^{-1} D_T\right)\right) \qquad (3.35)$$

$$|\alpha|^2 = 8 G^2 \cos^2\theta_c \left(\frac{(E+E')^2}{1 - q^2/4} + q^2\right) \left| F_V' + q \frac{F_V^2}{4M^2} \right|^2$$

$$|\beta x|^2 + |\beta y|^2 = 8 G^2 \cos^2\theta_c \left(\left[\frac{(E+E')^2}{1-q^2/4} - q^2\right]\left[\frac{-q^2}{4}\left|F_V' + \xi F_V^2\right|^2 + \left|F_A\right|^2\left(1 - q^2/4\right)\right] + 2\left(F_V' + \xi F_V^2\right) F_A\, q^2 (E+E')\right)$$

The exclusion factors $D_{S,T,L}$ obtained using harmonic oscillator wave functions are plotted in Fig. 15 and 16 for two cases.

The main differences between the shell model and the Fermi gas model are:

1. Spin effects are important in the shell model near $q^2 = 0$, as evidenced by the fact that $D_S \neq D_T \neq D_L$ and $d\sigma/dq^2\Big|_{q^2=0} \neq 0$ for symmetric (N=Z) nuclei except in the case of closed shells. These effects are

very sensitive to configuration-mixing and are probably greatly exaggerated in Fig. 15 and 16 where only the simplest configurations were used. However, for $Q^2 \gtrsim 0.02$ GeV^2 the three shell model exclusion factors are approximately equal and the choice of wave function is presumably not very important.

2. The shell model is much more dilute than the Fermi gas model (which is based on central, and not average, nuclear densities) and the exclusion effect is therefore less.

In the absence of detailed electromagnetic experiments on the quasi-elastic peak in nuclei we have no real reason to prefer one particular model and it is distressing that the models discussed here differ by $\sim 20\%$ for $Q^2 \sim 0.05 - .1$ GeV^2. We recommend trying both models and assigning errors to cover the difference.

Equations (3.34) and (3.35) can be applied to a deuterium target. A simple calculation gives

$$\left.\frac{\left(\frac{d\sigma}{dq^2}\right)_{\nu d}}{\left(\frac{d\sigma}{dq^2}\right)_{\nu n}}\right|_{q^2=0} = \frac{\frac{2}{3}\left(\frac{g_A}{g_V}\right)^2}{1+\left(\frac{g_A}{g_V}\right)^2} = 0.39 \qquad (3.36)$$

independent of the choice of space wave function (at $\vec{q}=0$ the vector current does not contribute since it does nothing but turn a neutron $\longleftrightarrow$ proton leading to a state which is forbidden by the Pauli principle; the axial current flips the spin in addition but its contribution is reduced since some states are forbidden). Block[B33] has calculated the exclusion factors in the closure approximation using a Hulthen wave function; he found that to $\sim \pm 1\%$ the deuterium/neutron cross section ratio is not sensitive to E_ν or to the choice of form factors. The ratio is shown in Fig. 17. Corrections to the closure approximation have not been studied.

The problem of neutrino scattering on deuterium (and nuclei) has recently been studied by Belavin and Gurvits[B4] who suggest that in certain configurations $(\sigma(\nu d)/\sigma(\nu n))$ should be equal to $\left(\sigma(\pi^+ d \longrightarrow p p \pi^o)/\sigma(\pi^+ n \longrightarrow p \pi^o)\right)$ to a good approximation. However, they do not take account of the vital spin effects which are different in the ν and π cases.

F. Experimental Results

Information about the quasi-elastic process has been obtained in both the bubble chamber[B45] and the spark chamber experiments[H5] at CERN and in a spark chamber experiment at ANL.[K15]

In the latter experiment obvious multiparticle events were eliminated but otherwise inelastic events could not be distinguished. After imposing various cuts to reduce the remaining inelastic background, it was allowed for by making a 10% overall subtraction (estimated assuming N* dominance and using the model of Berman and Veltman).*[B16] The results are shown in Fig. 18 and 19; the theoretical curve for free neutrons was obtained using CVC, $F^3_{V,A} = F_p = 0$ and a dipole fit for F_A with $M_A^2 = 0.71\ \text{GeV}^2$. The experiment is notable for the conspicuous absence of the exclusion effect which is especially surprising in view of its established effect in μ capture; this might be attributed to an incorrect allowance for inelastic events.

---

*The Berman-Veltman cross section agrees approximately with the available data but this may be fortuitous since they overestimated the vector couplings by a factor $\sqrt{3/2}$ due to a misinterpretation of a previous paper. With the correct vector couplings, their cross section is unchanged at $Q^2 = 0$ but reduced at large Q^2.

The CERN spark chamber group analyzed the events initiated in the Aℓ plates in essentially the same way. A dipole form was used for F_A and $M_A = 0.65\ ^{+0.45}_{-0.40}$ GeV was obtained from fitting the q^2 distribution of events with $E_\nu > 1.4$ GeV which is shown in Fig. 20 (this method is insensitive to the spectrum since $\sigma(E_\nu)$--Fig. 10--is approximately constant at this energy) and the angular distribution of all events.

In the CERN bubble chamber experiment it was easier to isolate the quasi-elastic process, background being estimated using Monte Carlo programs. Again CVC was used with $F_p = F^3_{V,A} = 0$ and a dipole form adopted for F_A. $M_A = 0.7 \pm 0.2$ GeV was obtained by fitting both $\sigma_\nu(E_\nu)$--Fig. 21--and the differential cross section (using a Fermi gas model)--Fig. 22. Exactly the same result was also obtained by taking the cross section for events with $Q^2 > 0.3$ GeV^2 where nuclear effects should be unimportant; in this case $E_\nu \gtrsim 1$ GeV and the shape of the spectrum is not important.

3.4. Quasi-elastic Neutrino Scattering ($\Delta Y = \pm 1$)

The most general forms of the currents in the processes $\nu(\bar{\nu})\, N \longrightarrow \ell^-(\ell^+) Y$ are the same as in the $\Delta Y = 0$ reactions [Eqs. (3.13) and (3.14)] except that $\cos\theta_c \longrightarrow \sin\theta_c$. T invariance again implies that all the form factors are relatively real. Unless the conventional theory fails badly at high energies it will be a long time before accurate measurements of $\Delta Y = 1$ cross sections are available and we shall therefore work in the approximation $m = 0$ in this section (the general case is given, e.g., in A2, P4). In this approximation the differential cross section